ELSEVIER

Journal of Nuclear Materials 249 (1997) 190–198

journal of nuclear materials

Radio-frequency sheath mitigation by insulating antenna limiters

J.R. Myra [a,*], D.A. D'Ippolito [a], J.A. Rice [b], C.S. Hazelton [b]

[a] *Lodestar Research Corporation, 2400 Central Avenue P-5, Boulder, CO 80301, USA*
[b] *Composite Technology Development, 1505 Coal Creek Dr., Lafayette, CO 80026, USA*

Received 10 March 1997; accepted 6 June 1997

Abstract

Previous work, undertaken in the low heat flux environment of small experiments, has shown that insulating limiters made out of boron nitride can enhance the performance of rf antennas by mitigating the rf voltages available to drive plasma sheaths. In the present study, we develop a quantitative model of rf sheath mitigation and apply it to determine the rf electrical specifications that a material should meet to be suitable as an insulating rf limiter. Additional properties of a suitable material are discussed and compared with the properties of commonly available materials and with newly developed ceramic matrix composite materials. It is concluded that an rf limiter made from composite materials looks promising for use in sheath mitigation, especially for fast wave antennas. © 1997 Elsevier Science B.V.

PACS: 52.40.Hf; 52.50.Gj; 81.05.Mh; 81.05.Je

1. Introduction

It is by now well established that the ion cyclotron range of frequency (ICRF) systems can heat fusion plasmas for a wide range of physics heating scenarios (see, for example, Ref. [1]) and efforts are well under way to employ ICRF systems for driving steady state current in tokamaks [2]. While ICRF systems can be made robust and effective, attention must be paid to certain critical ICRF, edge interaction issues. Experiments have shown that under adverse conditions, ICRF systems can lead to increased impurity injection from the antennas and/or their limiters into the plasma [3], the formation of 'hot spots' and arcs on the antenna surface [4], excessive power dissipation at the edge [4], non-linear loading [5,6] (i.e., loading that is a function of power) and modifications of the scrape off layer (SOL) plasma [3,7,8]. Many of these issues, while present during ICRF heating experiments, are expected to be even more important for extended current drive arrays, which fill a substantial fraction of the SOL volume and for which anti-symmetric (dipole, or $0-\pi$) phasing cannot be employed. Furthermore, recent developments in the ICRF launcher design for the international thermonuclear experimental reactor (ITER) suggest that there will be a need for 'in-port' designs capable of handling high voltages and power densities without breakdown, or severe impurity problems. It has been shown that many of these deleterious antenna–plasma interactions are caused by the formation of radio-frequency (rf) sheaths [9–12]. A great deal of recent work has been devoted to the study of rf sheaths on JET [4,13,14], TFTR [15,16], and other tokamaks [7,8,17] in order to design future ICRF antennas to minimize these effects.

Work begun at the University of Wisconsin [18–20] has recently demonstrated that the rf sheath problem on ICRF antennas could be greatly reduced by surrounding the antennas with protection limiters made of or coated with an insulating material. The basic idea (which will be discussed in more detail in Section 2) is that most of the induced voltage can be made to appear across the insulator instead of across the sheath when the condition $Z_{sh} < Z_{in}$ is met, where Z_{sh} and Z_{in} are the impedances of the sheath and insulator, respectively. The experiments on the Phaedrus-T tokamak at the University of Wisconsin used 1/4 inch thick boron nitride limiters and demonstrated substan-

* Corresponding author. Tel.: +1-303 449 9691; fax: +1-303 449 3865; e-mail: myra@lodestar.com.

PII S0022-3115(97)00210-9

tial reduction in the rf sheath and plasma self-bias effects. These experiments achieved much improved rf operation in terms of power handling and antenna voltage, minimal impurity influx and edge modifications and control of the plasma density during rf operation [18,19]. Detailed experimental results and modeling of the effects of the Faraday screen and the insulating side limiters on edge potentials, antenna loading, edge power dissipation and impurity behavior have recently been published [20]. Subsequent experimental work at the Princeton Plasma Physics Laboratory has also successfully employed boron nitride limiters on the ICRF antenna used to heat the CDX-U tokamak [21].

While boron nitride has demonstrated its usefulness in small present day experiments, it is not a very suitable material for use in long-pulse fusion experiments and reactors, because it is difficult to braze and suffers neutron damage. Additionally, it has a tendency to absorb and release water [21]. Furthermore, boron nitride has a tendency to undergo phase change from hexagonal to cubical structure under high (magnetic and kinetic) pressures and heat fluxes from plasmas. The cubic structure is not favorable when ablated in disruption events, as it is more abrasive [22]. Thus, there is motivation for developing insulating materials which are more fusion appropriate and can stand up to the harsh plasma environment in the vicinity of an rf antenna in a large experiment. In this paper, we review, in Section 2, the basis for the reduction of sheath voltages by the use of insulating limiters and develop a model which we then employ in Section 3 to determine the electrical specifications of an insulating rf-limiter material. In Section 4 we review thermal and other specifications of an ideal material and in Section 5 some candidate materials under development are discussed. Finally, the conclusions of the paper are given in Section 6.

2. Insulating rf-limiter and sheath model

As discussed by Majeski et al. [18,19], deleterious rf sheath interactions can be eliminated or greatly reduced by employing an insulator (or insulating coating) at the material boundary where the sheath would form. The basic circuit diagram employed here is illustrated schematically in Fig. 1. The reader is referred to Ref. [20] for examples of additional equivalent circuits that are useful in assessing the role of the rf sheath in antenna operation. The plasma sheath (subscript sh) and the insulator (subscript in) are both modeled as a resistance and capacitance connected in parallel. The sheath and insulator themselves are seen as series-connected impedances, so that the voltage drop across the sheath relative to the applied voltage is given by

$$\frac{V_{sh}}{V} = \frac{Z_{sh}}{Z_{sh} + Z_{in}}, \tag{1}$$

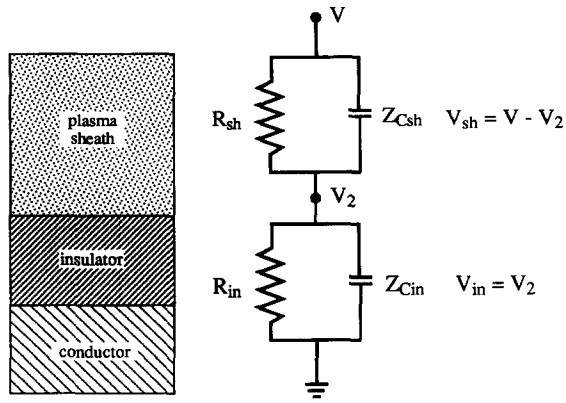

Fig. 1. Basic circuit diagram for sheath/insulator calculations.

where $1/Z_j = 1/R_j + 1/Z_{Cj}$ for j = sh or in and $V_{sh} = V - V_2$. Thus, V_{sh}/V varies from 0 to 1. Most of the voltage V can be made to appear across the insulator V_{in} instead of across the sheath V_{sh} when the condition

$$Z_{sh} \ll Z_{in} \tag{2}$$

is met. Here, we implicitly consider the behavior of the fundamental rf frequency (i.e., the frequency at which the antenna is driven). Sheath non-linearities also drive higher harmonic rf components, which are only partially modeled by the lumped circuit sheath model employed here. When Eq. (2) is well satisfied for the fundamental, it is also typically well satisfied for the harmonics of significant amplitude and insulator mitigation of the sheath voltage will occur.

For the insulator, the resistance is $R_{in} = \eta d/A$ where η is the effective ac volume resistivity, d is the thickness of the insulator and A is its surface area. The capacitive impedance of the insulator (in SI units) is $|Z_{in,C}| = d/\varepsilon\omega A$ where ε is the dielectric constant of the insulator and ω is the rf frequency. Explicitly, upon unit conversion, we have

$$R_{in}(\text{ohm})\, A(\text{m}^2) = \eta(\text{ohm m}) d(\text{m}), \tag{3a}$$

$$|Z_{in,C}|(\text{ohm})\, A(\text{m}^2) = 18 d(\text{mm})/[\, Kf(\text{MHz})], \tag{3b}$$

where $\omega = 2\pi f$ has been used and $K = \varepsilon/\varepsilon_0$. For typical insulating coatings of interest, $|Z_{in,C}| \ll R_{in}$, so that the dominant current channel through the insulator is capacitive [18,19] and Eq. (2) reduces to $Z_{sh} \ll d/\varepsilon\omega A$.

Because the sheath is governed by non-linear plasma physics [9–12], its representation in terms of lumped circuit elements is somewhat subtle. We consider a collisionless high voltage Child–Langmuir sheath which consists of an electron depleted (i.e., ion rich) layer of width $\Delta = \lambda_D(eV_{sh}/T)^{3/4}$ where $\lambda_D = (\varepsilon_0 T/n_e e^2)^{1/2}$ is the electron Debye length, T is the electron temperature, n_e is the electron density at the antenna, e is the electron charge and V_{sh} is that fraction of V that appears across the sheath, i.e., $V_{sh} = VZ_{sh}/(Z_{sh} + Z_{in})$. The capacitive impedance of the sheath is therefore approximately $|Z_{sh,C}| = \Delta/\varepsilon_0\omega A$.

The sheath also has a resistive component which is best understood in terms of sheath power dissipation. It has been shown [23] that the power dissipated in an rf sheath is given by

$$P_{sh} = An_e c_s Th(\xi)\xi I_1(\xi)/I_0(\xi). \quad (4a)$$

where $c_s = T/m_i$ is the sound speed, m_i is the ion mass, $\xi = eV_{sh}/T$, I_0 and I_1 are Bessel functions (which arise from the sheath-generated harmonics of the applied rf wave) and $h(\xi) = (0.5 + 0.3\xi)/(1 + \xi)$ is an order unity form factor as obtained in Ref. [23]. The resistance of the sheath is thus

$$R_{sh} = V_{sh}^2/2P_{sh}. \quad (4b)$$

In the small argument ($\xi < 1$, low sheath voltage limit) the result is $R_{sh} = 2T/An_e c_s e^2$ in agreement with Ref. [18], where the resistance was computed from the derivative of the $I(V)$ sheath characteristic. Converting units, we have

$$R_{sh}(\text{ohm})\,A(\text{m}^2) = 3.8 \times 10^{14} V_{sh}(\text{volt}) / \left[n_e(\text{m}^{-3})T(\text{eV})^{1/2}\right], \quad eV_{sh} \gg T, \quad (5a)$$

$$R_{sh}(\text{ohm})\,A(\text{m}^2) = 6.4 \times 10^{14} T(\text{eV})^{1/2}/n_e(\text{m}^{-3}), \quad eV_{sh} \ll T, \quad (5b)$$

$$|Z_{sh,C}|(\text{ohm})\,A(\text{m}^2) = 18\Delta(\text{mm})/f(\text{MHz}). \quad (5c)$$

For typical parameters applicable to the ICRF sheath ($T =$ 25 eV, $n_e = 10^{18}$ m^{-3} at the sheath entrance near the tips of the limiter, $V_{sh} = 1000$ V, $\Delta = 0.37$ mm, $f = 50$ MHz) we find that R_{sh} and $|Z_{sh,C}|$ are comparable and $Z_{sh}A$ is on the order of 0.1 Ω m^2.

A convenient, though conservative, requirement for reducing the rf sheath voltage is given by employing the capacitive limits for both insulator and sheath impedance in Eq. (2) to obtain $d \gg K\Delta$ as the required thickness of insulating material. For the above sample parameters (and employing $K \sim 5$–10), this requirement suggests that an insulating coating would have to be several mm, perhaps even up to 10 mm, thick. As V_{sh} is reduced, however, and the low voltage form of R_{sh} starts to apply, the requirement on d becomes less stringent. A more accurate specification of this requirement and a quantitative evaluation of the relationship of insulator and plasma parameters to the sheath voltage mitigation that is achieved by the use of insulating limiters is the subject of Section 3.

3. Numerical results for the electrical specifications of an rf-limiter

In this section, we summarize the requirements for rf insulators as calculated numerically by a code which solves the preceding sheath insulator circuit equations. Specifically, the code solves for V_{sh}/V given by Eq. (1), using

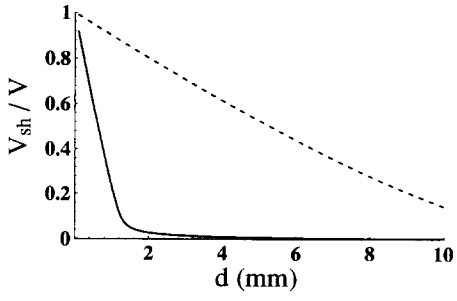

Fig. 2. Effectiveness of insulator mitigation of sheaths with insulator thickness d for driving voltages of 1 (solid curve) and 10 kV (dashed curve).

Eqs. (3a), (3b), (4a), (4b) and (5c). Since the sheath circuit elements are non-linear, i.e., Eqs. (4b) and (5c) give R_{sh} and $Z_{sh,C}$ as functions of V_{sh} itself (through Δ and ξ), the procedure involves numerial rootfinding to determine V_{sh} for a specified value of V. Thus, the code solves the non-linear rf circuit equations that describe the split-up of rf voltage between a plasma sheath and the insulator. The goal is to calculate the required insulator parameters, thickness d, dielectric constant ε and resistivity η, such that the insulator takes a large fraction of the rf voltage that would otherwise appear across a plasma sheath. The important plasma parameters that can be varied in this model are the electron plasma density n_e and temperature T_e at the antenna and the rf parameters are the frequency f and the voltage V. We consider that the insulators are nominally working when $V_{sh}/V < 0.1$. An exception to this criterion (that occurs for parameters when even large sheaths are inconsequential) will be discussed later.

Figs. 2–6 show the variation of V_{sh}/V as a function of the various plasma and insulator parameters. The parameters are varied about a base case, unless otherwise indicated, which is taken as $d = 10$ mm, $K = 7.7$, $\eta = 10^8$ Ω m, $f = 50$ MHz, $T_e = 25$ eV and $n_e = 10^{18}$ m^{-3}. Also, the plasma is deuterium (ion mass $\mu = 2$) and two rf voltages are shown, $V = 10$ and 1 kV. The 1 kV case is nominally a worst case for fast wave (FW) antenna sheaths. In certain

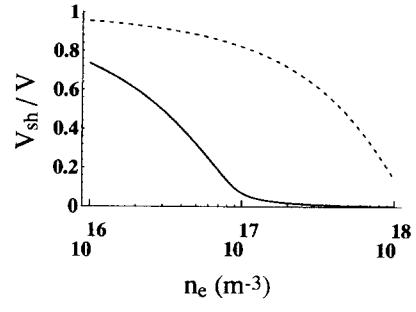

Fig. 3. Effectiveness of insulator mitigation of sheaths with plasma density at the antenna n_e for driving voltages of 1 (solid curve) and 10 kV (dashed curve).

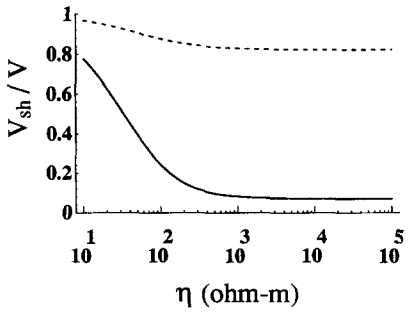

Fig. 4. Effectiveness of insulator mitigation of sheaths with insulator resistivity η for driving voltages of 1 (solid curve) and 10 kV (dashed curve). This plot is done for a plasma density of $n_e = 10^{17}$ m^{-3} rather than for the base case plasma density $n_e = 10^{18}$ m^{-3}.

extreme cases of FW operation, such as very badly misaligned Faraday screens, several kV may be possible. The 10 kV case is mostly of pedagogical interest for FW antennas, but is the correct order of magnitude for sheath voltages in the case of ion Bernstein wave (IBW) antennas, where the rf electric field is excited with a polarization that is parallel to the equilibrium magnetic field of the tokamak.

In Fig. 2 we consider the variation of V_{sh}/V with insulator thickness d. For base case parameters, an insulator thickness of $d = 10$ mm is adequate to mitigate rf driving voltages up to 10 kV. For the FW (1 kV) case, a much thinner insulating layer of about 1 mm would suffice.

Fig. 3 shows that when the plasma density is reduced from its base case value of $n_e = 10^{18}$ m^{-3} the insulator is less effective in mitigating the sheaths. This occurs because the sheath resistance and capacitance are functions of n_e. For the 1 kV case, the density must be nearly 10^{17} m^{-3} or more to achieve a 10:1 reduction in V_{sh}/V; for the 10 kV (IBW) case sheath voltage mitigation is essentially not possible for densities less than 10^{18} m^{-3}. However, it must also be noted that sheaths are less of a concern at low plasma density because most of the deleterious sheath

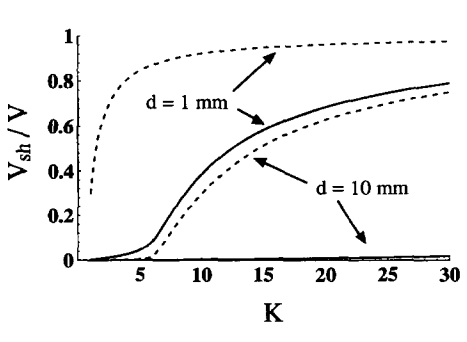

Fig. 5. Effectiveness of insulator mitigation of sheaths with insulator dielectric constant K for driving voltages of 1 (solid curves) and 10 kV (dashed curves). Results for two different values of thickness d are indicated.

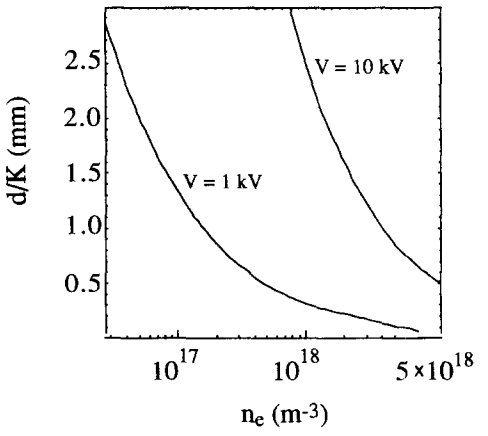

Fig. 6. Contours of $V_{sh} / V = 0.1$ for $V = 1$ and 10 kV. Above the indicated contours, $V_{sh} / V < 0.1$ pertains, and the sheath mitigation is regarded as successful.

phenomena (e.g., sheath power dissipation and impurity sputtering) are proportional to n_e. It might be hoped that at low n_e sheath effects can be neglected and that at high n_e the insulators do their job to reduce V_{sh}. We shall return to this point later.

Next, we explore the role of the insulator resistivity η. As mentioned in the discussion of Eqs. (3a) and (3b), typical insulator resistivities are sufficiently large that the dominant current channel through the insulator is normally capacitive (i.e., dominated by the displacement current). This gives some latitude in the choice of η. This freedom can be exploited to optimize the other desired properties of the material. Consequently, it is interesting to obtain bounds on the allowed values of η. In Fig. 4 we show V_{sh}/V versus $\log_{10}(\eta)$ at a plasma density of $n_e = 10^{17}$ m^{-3}. (At the base case density of $n_e = 10^{18}$ m^{-3}, both curves would be essentially zero.) The figure shows that the results are independent of insulator resistivity η, down to a value of about 10^2 to 10^3 Ω m, depending on V. When the effective resistivity η is dominated by ac effects, as is frequently the case, ($\eta_{ac} = 1/\omega\varepsilon \tan\delta$, where $\tan\delta$ is the loss tangent) this implies a limit on $\tan\delta$, which is approximately $f(\text{MHz})K \tan\delta < 36$, in order for the sheath mitigation to be insensitive to, and not degraded by, ac losses.

Finally, we consider the sensitivity of the results to the relative dielectric constant of the insulator, K. Fig. 5 shows V_{sh}/V versus K for two different values of thickness, $d = 10$ mm and $d = 1$ mm. The plots show, as expected, that a larger dielectric constant is disadvantageous because it decreases the capacitive impedance of the insulator and therefore forces a greater fraction of the voltage drop to appear across the sheath. Insulators with $K < 8$ or so would appear to be acceptable in all but the most severe case, that of a 10 kV driving voltage with $d = 1$ mm. For the interesting situation of driving voltage, $V \leq 1$ kV and $d \sim 10$ mm, there is essentially no restriction on K.

When η is large (so that the results are independent of η) d and K enter the model only in the combination d/K. This enables the parametric dependencies to be summarized in a contour plot in terms of the important parameters d/K and plasma density n_e. This is illustrated in Fig. 6. Above the contours V_{sh}/V is less than 0.1, so according to our nominal criterion, in this region of the plot the insulators are greatly beneficial. The lower curve is for $V = 1$ kV and the upper one for $V = 10$ kV. Again, we note that the insulators do not provide much relative mitigation at the lower values of n_e and this point is addressed next. Note again that rather thick coatings or very small K materials are required to make the idea work in the IBW case.

At low n_e the insulators are not as effective in mitigating sheath voltage, but neither are sheaths so dangerous. To illustrate this point, in Fig. 7 we plot the sheath power dissipation P_{sh} from Eq. (4a) as a function of n_e. In the uppermost curve ($V = 10$ kV and $d = 1$ mm) the insulators provide no mitigation and the linear dependence of P_{sh} on n_e is evident. For the parameters employed, the sheath power dissipation is nearly a MW at $n_e = 10^{18}$ m^{-3}, which would be devastating. For the other cases, P_{sh} rolls over at some density that is sufficiently high to allow the insulator impedance to exceed the sheath impedance. When P_{sh} is an issue (i.e., when it exceeds a few tens of kW or so) the maximum in P_{sh} occurs for $n_e > 3 \times 10^{17}$ m^{-3}, so it is reasonable to design the insulator to achieve significant mitigation ($V_{sh}/V < 0.1$) for n_e at least this large. At lower n_e sheath problems will be better, not worse.

For the above cases, we assumed an area of $A = 0.01$ m^2 (surface area of the insulator and sheaths) so it is also interesting to note that the power flux reaches 10 MW/m^2 (considered to be a practical upper design limit) when $P_{sh} = 10^5$ W, which also occurs only in the high density limit.

4. Thermal and other specifications

A candidate insulating material must be able to survive the heat and neutron flux in a fusion environment and to withstand the large induced voltages in the vicinity of ICRF antennas. In addition, to be useful in fabricating a coating or jacket for an antenna limiter, the material must have certain mechanical properties. A discussion of these properties is the subject of the present section.

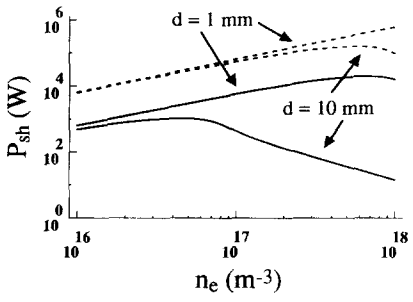

Fig. 7. Dependence of sheath power dissipation P_{sh} on plasma density n_e for driving voltages of 1 (solid curve) and 10 kV (dashed curve). Results for two different values of thickness d are indicated. The assumed area of the sheaths is $A = 0.01$ m^2.

The primary thermal requirement on the insulator is that it be able to withstand a (long pulse) heat load Q up to $Q = 10$ MW/m^2 without overheating and sublimation. For a sample of thickness d, this means that in steady state the change in temperature, ΔT, across the insulator and the thermal conductivity, κ, are related by $\kappa \Delta T = Qd$. Thus the maximum temperature that the insulator can withstand T_m and its thermal conductivity must satisfy

$$\kappa T_m \geq Qd, \tag{6}$$

where $T_m \approx \Delta T$ is assumed. For a $d = 10$ mm sample and a typical T_m of order 1000 K, the required κ is about 100 W/m · K. Designing for $Q = 10$ MW/m^2 would be considered conservative, since the antenna limiters should not generally be subject to such intense heat fluxes; a nominal steady-state heat flux would not exceed 5 MW/m^2. Furthermore, the normal Bohm diffusion driven heat flux is typically a factor of 10 or more smaller and if the insulators perform efficiently with regard to sheath mitigation (and hence sheath-driven heat flux), Q should remain well below even the 5 MW/m^2 level, except perhaps during short pulses if the antenna limiters are subject to a plasma disruption. Disruption is a worst case scenario that might impose several GW/m^2 heat flux over a short period of 0.1–0.2 ms.

A suitable material will also behave well with respect to outgassing, maintaining a low equilibrium vapor pressure (less than 10^{-6} Torr) for temperatures of order 1000–1500°C. The critical temperature with respect to thermal shock resistance should be 1000°C or more.

The rf losses in the material should be negligible, both when compared with the launched power, and when viewed as a heat source for Joule heating the insulator. For the types of highly insulating materials that we are considering, the fields penetrate without substantial attenuation and the power dissipation in a volume $\mathscr{V} = Ad$ is given by

$$P = \langle \boldsymbol{J} \cdot \boldsymbol{E} \rangle \mathscr{V} = \omega \varepsilon \tan \delta |E|^2 Ad/2$$
$$= 2.78 \times 10^{-5} fK \tan \delta |E|^2 Ad, \tag{7}$$

where in the final form the units are P (W), f (MHz), E (V/m), A (m^2) and d (m), $f = 2\pi\omega$ is the frequency and $\tan \delta$ is the loss tangent of the insulator. In obtaining Eq. (7) we have used the relationship $\sigma = \omega \varepsilon \tan \delta$ where σ is the ac conductivity. When high voltage sheaths are being mitigated, the electric field in the insulator could be large, $E \sim 100$ kV/m. Employing this value and $f = 100$ MHz (a worst case), $A = 4 \times 10$ mm $\times$ 1 m, $d = 20$ mm (for four 'picture frame' limiters with radial dimension d surrounding a 1 m^2 antenna), $K = 7.7$ and $\tan \delta = 0.04$ (see Table 1), yields $P = 6.8$ kW as a representative number, compared with a typical total launched power of 1

Table 1
Physical properties of composite limiters

Material	Density (kg/m^3)	Open porosity %
CMC-A	2560	0.2
CMC-B	2810	0.2
CMC-C	2770	0.2

MW per antenna. For FW antennas, this is probably an upper bound because E as large as 100 kV/m is unlikely to exist throughout the entire insulator volume. To put this power in perspective, we note that it will heat the limiters by an amount equivalent to a heat flux from the plasma of only $Q \sim P/A = 0.17$ W/m^2, well within our design goals. On the other hand, if 1 MV/m fields were to exist throughout the insulator volume (as could be imagined in a worst case IBW scenario) the Joule heating would be an unacceptable $P = 680$ kW (a significant fraction of the launched power) and equivalent to $Q = 17$ MW/m^2. Even if the 1 MV/m fields were confined to a small local volume so that the total power loss was negligible, the resulting local heating of the insulator would still be problematic.

The insulating limiters must also be able to withstand the rf voltage that would have otherwise appeared across the sheath, without dielectric breakdown. Typical rf voltages will be in the range of a few hundred volts up to perhaps ten kilovolts. Thus, in the worst case, the dielectric breakdown field of the material must obey

$$E_{\mathrm{dbd}} > 10\ \mathrm{kV/d}. \tag{8}$$

Even for a sample as thin as 1 mm, the above condition should not be difficult to satisfy. Typically, we envision $V \sim 1$ kV and $d \sim 5$ mm (to meet the electrical requirement of Section 3), so E_{dbd} need only exceed 0.2 kV/mm.

Some secondary issues which impact the material's suitability in a fusion environment, but are not directly critical to the underlying idea of sheath mitigation, are that it be not overly hydroscopic and not embrittled by neutrons. It should have the mechanical strength necessary to handle disruption forces and ablation thresholds to minimize surface vaporization and should be able to be machined or fabricated easily. Sputtering and radiation enhanced sublimation must be acceptable, with any sputtered material having a low average Z (atomic number) and not too much oxygen content (to avoid chemical sputtering problems). The insulator should not overly absorb and retain gas, and finally it should have suitable secondary electron emission properties. These issues have not been quantified with respect to rf limiter specifications in the present study, but remain a topic of study for future work. Some comments on secondary electron emission and sputtering follow.

Secondary electron emission [24] has been neglected in the present modeling for simplicity. In the (unbiased) situation usually discussed in the literature, this effect reduces the plasma floating potential relative to the wall by an amount of order $T_e \ln(1-\gamma)$, where γ is the secondary emission coefficient. [25] In some cases $\gamma \sim 1$ can result in space charge saturation of the sheath voltage drop. [26] However, for an rf *driven* sheath with $eV_{\mathrm{sh}} \gg T$, it is not expected that secondary electron emission can substantially modify the sheath voltage drop, which must always be of order of the voltage applied to the plasma. When insulating limiters are successfully employed to reduce V_{sh} from the kV level down to 100 V or less (i.e., down to the level of a few T_e) secondary electron emission may play a role in distinguishing among several candidate insulating materials. In terms of the present model, secondary electron emission would modify the low voltage limit of sheath dissipation in Eq. (5b), and the corresponding dc sheath voltage drop $\langle V_{\mathrm{sh}} \rangle$ discussed in Ref. [23].

The stated goal of this work has been to reduce the sheath voltage, partly in order to reduce sputtering of impurities from the antenna into the plasma, which at low energies increases with ion impact energy and hence with sheath voltage. (Reduction of sheath power losses and other edge interactions such as arcing are also reasons for reducing V_{sh}.) At sufficiently high energies, the sputtering yield Y can maximize and begin to decrease with energy [27]. It might be thought that in this regime mitigation of high voltage sheaths would be detrimental rather than beneficial, however this is not normally thought to be the case. Both the erosion of the antenna and the impurity flux into the plasma scale as the product $Y\Gamma$ where Γ is the flux of plasma into the antenna. For large sheath voltages, Γ is dominated by the process of $E \times B$ convection, [28] where E is the dc electric field resulting from the rectified sheath voltage. The product $Y\Gamma$ is most often an increasing function of V_{sh} in regimes of interest, although this point deserves further attention specific to the candidate materials that are to be developed as insulating limiters.

5. Discussion of candidate materials

Recent progress in materials development has revealed some promising candidate composite materials from which an acceptable rf-insulating limiter might be constructed. The class of materials that has been investigated are ceramic matrix composite (CMC) materials fabricated with both high performance ceramic fibers and high thermal conductivity particulate fillers.

Various techniques exist for fabricating ceramic composites including chemical vapor infiltration (CVI) or chemical vapor deposition (CVD), carbon to SiC conversion, hot pressing and hot isostatic pressing of powders, metal oxidation and preceramic polymer conversion. CVI is currently the most common method for producing fiber reinforced components. However, CVI is a slow and ex-

Table 2
Electrical properties of composite limiters (dielectric properties measured at 1 MHz)

Material	Dielectric constant, K	Loss tangent, $\tan\delta$	Bulk resistivity (Ω m)
CMC-A	6.27	0.0061	7.9×10^{9}
CMC-B	7.76	0.044	$4.7\times\times10^{9}$
CMC-C	6.35	0.041	9.7×10^{8}

pensive process, which usually produces conductive or semiconductive parts. Polymer infiltration processing (PIP) of preceramic polymers can overcome many of the disadvantages of CVI and should be investigated for fusion applications.

PIP offers the advantage of ceramic properties through polymer-like processing. Near net shape fabrication can be achieved with resin transfer molding, prepreg autoclaving, or injection molding. The polymeric matrix is then cured and pyrolyzed in an inert atmosphere transforming it into the ceramic matrix. To achieve full densification (up to 95–98% theoretical density and 2 to 8% open porosity) the composite is re-infiltrated and pyrolyzed 3 to 6 times. The part is heat treated at higher temperatures to obtain full or maximum crystallinity. Several commercial non-oxide matrix compositions are available including amorphous Si–O–C and Si–O–N, crystalline Si_3N_4 and crystalline SiC [29]. The final composition can be tightly controlled to achieve high electrical resistivity, low porosity, and high strength. The matrix chosen for this early development effort is an amorphous Si–O–C polymer that transforms into a hard, strong ceramic phase with only a few percent of oxygen. Three different fillers were chosen from ceramic powders with high thermal conductivity and low electrical conductivity. Composites fabricated from these fillers are identified as CMC-A, CMC-B and CMC-C. Details of the materials and processing will be published in a separate paper [30].

During this preliminary development study, many material properties were measured, including physical properties, dielectric constant and loss tangent, and thermal conductivity. Test sample plates were fabricated and completely processed. Table 1 lists the density and open porosity levels achieved on three of the composite systems. As can be seen, all these samples have very low porosity. At this low level, moisture absorption from the atmosphere and outgassing in the vacuum environment should be negligible. The difference in the density (kg/m^3) is directly related to the difference in the density of the starting filler powders and the volume fraction. Table 2 lists the electrical properties that were measured. The dielectric constant of 6 to 7.7 is low and within the acceptable range of values calculated by the computer model. In future work, the optimization of the processing will be continued which should lower these values to near 5. Also, all of these materials exceed the bulk resistivity criteria (10^3 Ω m) by several orders of magnitude.

It is useful to compare the properties of any proposed material with other materials that have been used in an rf environment in fusion machines. Examples are boron nitride (which has some important limitations discussed in the introduction), boron carbide and graphite. Also of interest for the comparisons are other materials that are used in fusion, though not in an rf environment, such as carbon–carbon composites. A comparative summary of relevant electrical, thermal and mechanical properties is shown in Table 3.

Table 3
Comparison of relevant rf electrical, thermal and mechanical properties for some common fusion materials and for candidate CMC materials

	Conventional rf limiters			Plasma facing materials	Novel insulating composites		
	BN [31]	B_4C [32]	graphite [33]	carbon–carbon [33]	CMC-A	CMC-B	CMC-C
rf electrical							
Resistivity, η (Ω m)	$>10^{13}$	<10	c	c	8×10^{9}	5×10^{9}	1×10^{9}
Dielectric constant, K	4.1	c	c	c	6.3	7.8	6.4
Dielectric breakdown (kV/mm)	54	c	c	c	14.2	12.5	9.7
Thermal							
Thermal conductivity, κ (W/mK)	23–28	35	115	200–350	3–10	7–30	10–50
Mechanical							
Hardness	soft	very hard	hard	hard	hard	hard	very hard
Flexural strength (MPa)	20	350	NA	48	NA	NA	NA
Density (kg/m^3)	1900	2500	NA	1520	2770	2560	2810
Porosity (%)	13	<2	NA	<20	0.3	0.2	0.2

c = conductive sample, NA = data not available.

From Table 3 it is evident that the candidate CMC materials do compare favorably with more conventional materials typically used in the fusion environment. The electrical, chemical and physical properties meet or exceed all the primary specifications outlined above. Future development will concentrate on increasing the thermal conductivity and thermal shock resistance as well as improving manufacturability. Thus, at the present stage of development, it appears likely that sheath mitigation by insulating rf limiters should be possible using advanced CMC materials.

6. Conclusions

In this paper, we have presented a numerical model for assessing the mitigation of rf sheaths by the use of insulating limiters. The model has been employed to determine the specifications required of an insulating material for use as a limiter on both typical fast wave and ion Bernstein wave antennas. If the dielectric constant of the insulator is no more than $K = 8$, we find (from Fig. 6) that a thickness of about $d = 5$ mm is adequate to mitigate sheaths when the driving voltage is as high as $V = 1$ kV at a plasma density of $n_e = 3 \times 10^{17}$ m^{-3}. This should be suitable for application to typical fast wave systems, where the density at the tips of the limiter (closest to the plasma) is typically of order 10^{18} m^{-3} and falls off to values of order 10^{16}–10^{17} m^{-3} at the antenna Faraday screen. The density of $n_e = 3 \times 10^{17}$ m^{-3} was found to be approximately a worst case situation: at higher densities the insulator mitigation of sheaths is more effective, at lower densities, sheaths were found to be less of a concern (see Fig. 7).

For the IBW case, it was found that insulator mitigation of sheaths is more demanding. Typically, IBW antennas have larger sheath voltages and operate at lower densities. Both circumstances make sheath mitigation more difficult. If the IBW antennas were to operate at a density as high as 10^{18} m^{-3}, Figs. 2 and 3 indicate that the required insulator thickness is approximately $d = 10$ mm or perhaps a little more for $K = 7.7$. One speculation for why IBW antennas have not operated well at high edge plasma densities in the past is because of the sheaths. If the insulator mitigation of sheaths is successful at $n_e = 10^{18}$ m^{-3}, IBW operation may be possible at these high densities, whereas without sheath mitigation it was impossible. This lends a kind of self-consistency to the high density sheath mitigation regime. However, for this scheme to work, insulator materials with a small loss tangent and/or high thermal conductivity would be required to avoid difficulties with Joule heating of the insulator.

In order to further advance the ideas presented in this paper, a proof of principle experiment employing the new CMC insulators will be required. Boron nitride insulating limiters have already been employed with some success in the low heat flux environment of small experiments, and it is hoped that the superior properties of the CMC insulators indicated in Table 3 will result in further enhancements of antenna operation.

Acknowledgements

The authors wish to thank R. Majeski and D. Hoffman for useful discussions on materials requirements. The authors are also grateful to the referees for making several valuable comments, especially with regard to the properties of boron nitride. This work was supported by contract number DE-FG03-96ER82145 with the US Department of Energy.

References

[1] Proc. 10th APS Topical Conf. on Applications of Radio-Frequency Power to Plasmas, Boston, MA (American Institute of Physics, New York, 1994) pp. 3–80.
[2] R.I. Pinsker, AIP Conf. Proc. 289 (1994) 179.
[3] M. Bures, J. Jacquinot, A. Kaye, H. Brinkschulte, K.D. Lawson, J.A. Tagle, Plasma Phys. 30 (1988) 149, and Refs. therein.
[4] M. Bures, J.J. Jacquinot, M.F. Stamp, D.D.R. Summers, D.F.H. Start, T. Wade, D.A. D'Ippolito, J.R. Myra, Nucl. Fusion 32 (1992) 1139.
[5] the DIII-D Group, R.I. Pinsker, F.W. Baity, S.C. Chiu, J.S. DeGrassie, C.B. Forest, H. Ikezi, M. Murakami, C.C. Petty, R. Prater, D.W. Swain, AIP Conf. Proc. 355 (1996) 43.
[6] D.W. Swain, R.I. Pinsker, F.W. Baity, M.D. Carter, J.S. deGrassie, E.J. Doyle, G.R. Hanson, K.W. Kim, R.A. Moyer, C.C. Petty, Nucl. Fusion 37 (1997) 211.
[7] J.-M. Noterdaeme, AIP Conf. Proc. 244 (1992) 71.
[8] R. Van Nieuwenhove, G. Van Oost, P.E. Vandenplas, R.A. Moyer, D. Gray, R.W. Conn, Fusion Eng. Design 12 (1990) 231.
[9] F.W. Perkins, Nucl. Fusion 29 (1989) 583.
[10] R. Van Niewenhove, G. Van Oost, J. Nucl. Mater. 162–164 (1989) 288.
[11] R. Chodura, Fusion Eng. Des. 12 (1990) 111.
[12] J.R. Myra, D.A. D'Ippolito, M.J. Gerver, Nucl. Fusion 30 (1990) 845.
[13] D.A. D'Ippolito, J.R. Myra, M. Bures, J. Jacquinot, Plasma Phys. Cont. Fusion 33 (1991) 607.
[14] M. Bures, J. Jacquinot, K. Lawson, M. Stamp, H.P. Summers, D.A. D'Ippolito, J.R. Myra, Plasma Phys. Contr. Fusion 33 (1991) 937.
[15] R. Majeski, D.A. D'Ippolito, Y.L. Ho, J. Hosea, S. Medley, M. Murakami, J.R. Myra, C.K. Phillips, J.H. Rogers, G. Schilling, J. Stevens, G. Taylor, J.R. Wilson and the TFTR Group, in: Proc. 20th European Physical Society Conf. on Controlled Fusion and Plasma Physics, Vol. 17C, part III, Lisbon, European Physical Society, 1993, p. 977.
[16] D.A. D'Ippolito, J.R. Myra, R. Majeski, J.R. Wilson, Bull. Am. Phys. Soc. 39 (1994) 1627.
[17] J.-M. Noterdaeme, G. Van Oost, Plasma Phys. Contr. Fusion 35 (1993) 1481.

[18] R. Majeski, P.H. Probert, T. Tanaka, D. Diebold et al., Fusion Eng. Design 24 (1994) 159.
[19] R. Majeski, P.H. Probert, T. Tanaka et al., AIP Conf. Proc. 244 (1992) 322.
[20] J. Sorensen, D.A. Diebold, R. Majeski, N. Hershkowitz, Nucl. Fusion 36 (1996) 173.
[21] J. Menard, W. Choe, R. Majeski, M. Ono, D. Stutman, J.R. Wilson, T. Seki, Bull. Am. Phys. Soc. 41 (1996) 1402, paper 2R16.
[22] M.A. Bourham, J.G. Gilligan, Fusion Technol. 26 (1994) 517.
[23] D.A. D'Ippolito, J.R. Myra, Phys. Plasmas 3 (1996) 420.
[24] E.W. Thomas, in: Data Compendium for Plasma–Surface Interactions, Nucl. Fusion Special Issue 1984, International Atomic Energy Agency, Vienna, 1984, p. 94.
[25] P.C. Stangeby, G.M. McCracken, Nucl. Fusion 30 (1990) 1225, see section 3.3.
[26] C.A. Ordonez, Phys. Rev. E55 (1997) 1858, and references therein.
[27] J. Bohdansky, in: Data Compendium for Plasma–Surface Interactions, Nucl. Fusion Special Issue 1984, International Atomic Energy Agency, Vienna, 1984, p. 61 and errata in Nucl. Fusion 24 (1984) 1683.
[28] D.A. D'Ippolito, J.R. Myra, Phys. Fluids B5 (1993) 3603.
[29] D.W. Frietag, E.I. Aly, R.O. Scott, Preceramic Polymer Derived Ceramic Matrix Composites for Low Cost Aircraft Hot Structure, presentation notes, LTV Aerospace and Defense Company, Dallas, Texas.
[30] J.A. Rice, C.S. Hazelton, J.R. Myra, D.A. D'Ippolito, Ceramic Composite Insulators for Radio-Frequency Antenna Limiters, presented at the 99th Annual Meeting of the American Ceramic Society, Cincinnati, Ohio, May 4–7, 1997 and to be published in J. Nucl. Mater.
[31] Product literature, grade HBC and similarly grade HBT, Advanced Ceramics Corporation, Cleveland, OH, USA.
[32] Product literature, ESK Engineered Ceramics, Norwalk, CT, USA.
[33] L. Snead, T. Burchell, ORNL irradiation effects program, in: Proc. US–Japan Workshop Q-181 on High Heat Flux Components and Plasma–Surface Interactions for Next Devices, Sandia National Laboratories, 1994.